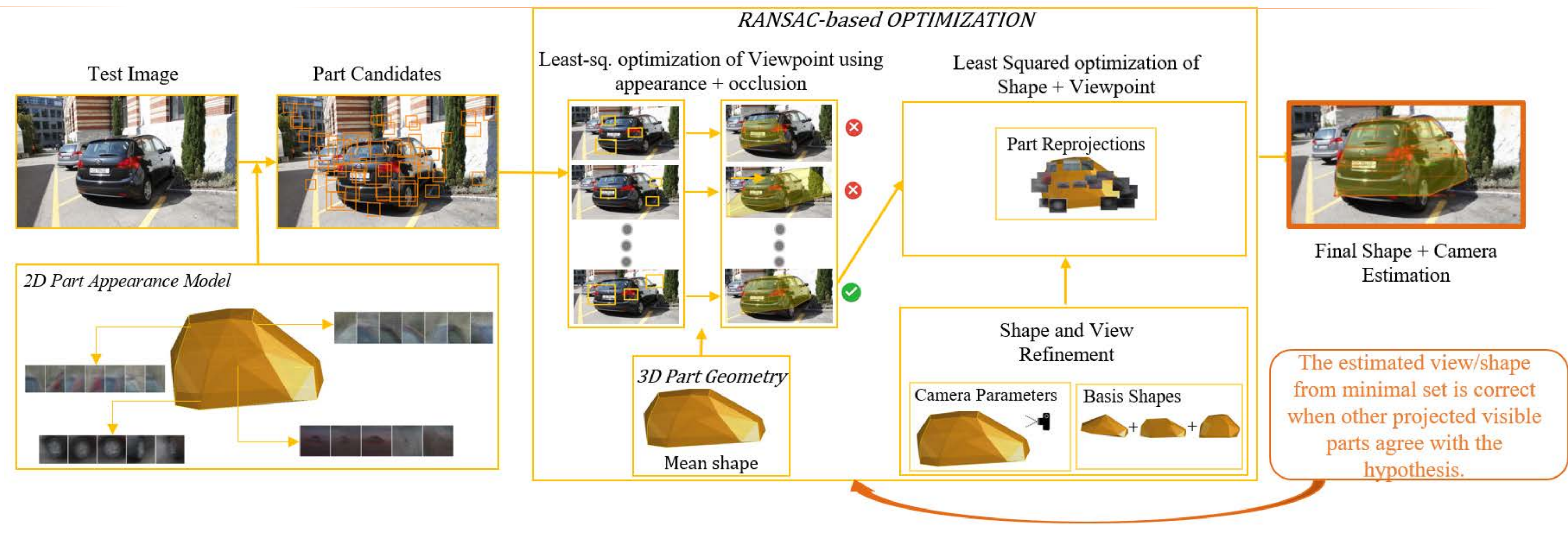


## GOAL

Class-specific reconstruction, viewpoint estimation and detection

- Deformable linear subspace, fine-grained, part-based model
- learnt from real image sequences (*no CAD models*)
- Geometric occlusion - cognizant reasoning (analytic optimization of shape + view with RANSAC) instead of regression.



## MODEL

• A Shape  $S = [s_1 \dots s_p]$  represents  $P$  semantic 3D parts on object shape instance, s.t.

•  $S = \sum_{l=1}^L \alpha_l B_l$  represents deformation in a linear subspace of  $L$  basis shapes learnt from training.

• The 2D projection of a 3D part location  $s_p$  is given as:

$$\hat{x} = \rho(C \cdot S_p) = \rho\left(C \sum_{l=1}^L \alpha_l b_{lp}\right)$$

• The loss function for computing Shape  $S$  and camera matrix  $C$  from visible image information:

$$L(\{\alpha_l\}, C) = \sum_{p=1}^P v(s_p, C) \cdot \|x_p - \rho(C \cdot s_p)\|^2, \quad s_p = \sum_{l=1}^L \alpha_l b_{lp}$$

where  $v(s_p, C) \in \{0, 1\}$  is binary visibility of  $s_p$  in camera  $C$ .

• This paper: Minimize  $L$  w.r.t. the shape coefficients  $\{\alpha_l\}$  and projection parameters  $C$ , using occlusion-aware, analytic optimization in a RANSAC framework.

## RELATED WORK

- [Pepik et al. ECCV 12] "3D2PM – 3D Deformable Parts Model"
- [Hejrati et al. CVPR 14] "Analysis by Synthesis"
- [Tulsiani et al. CVPR 15] "Viewpoints and Keypoints"
- [Zia et al. PAMI 13, CVPR 14]

*Most methods learn from labour-intensive CAD models (using similar models for result rendering too), often resorting to prediction using regression, ConvNets or sampling-intensive inference. We show the power of a simpler, automatic image-data-driven approach, that interleaves analytic optimization of geometric + deformation + occlusion properties with a RANSAC scheme.*

## DATASET

• *RealCar dataset*: 35 image sequences (between 30 and 115 images per sequence), taken around unique and distinct instances of cars, with challenging viewing conditions.

• *SfM (123DCatch)* is used to estimate the 3D car shapes and full camera matrices.

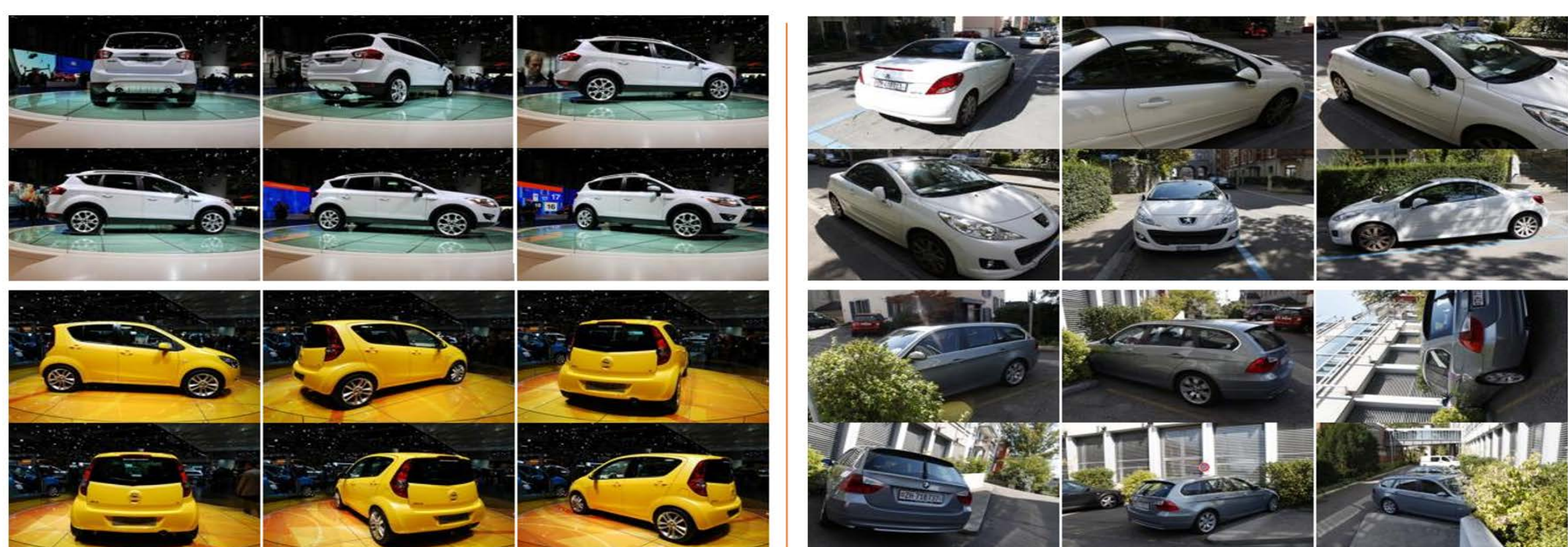


Figure 2: Examples from the EPFL Multi-view (Left) and our RealCar dataset (Right).

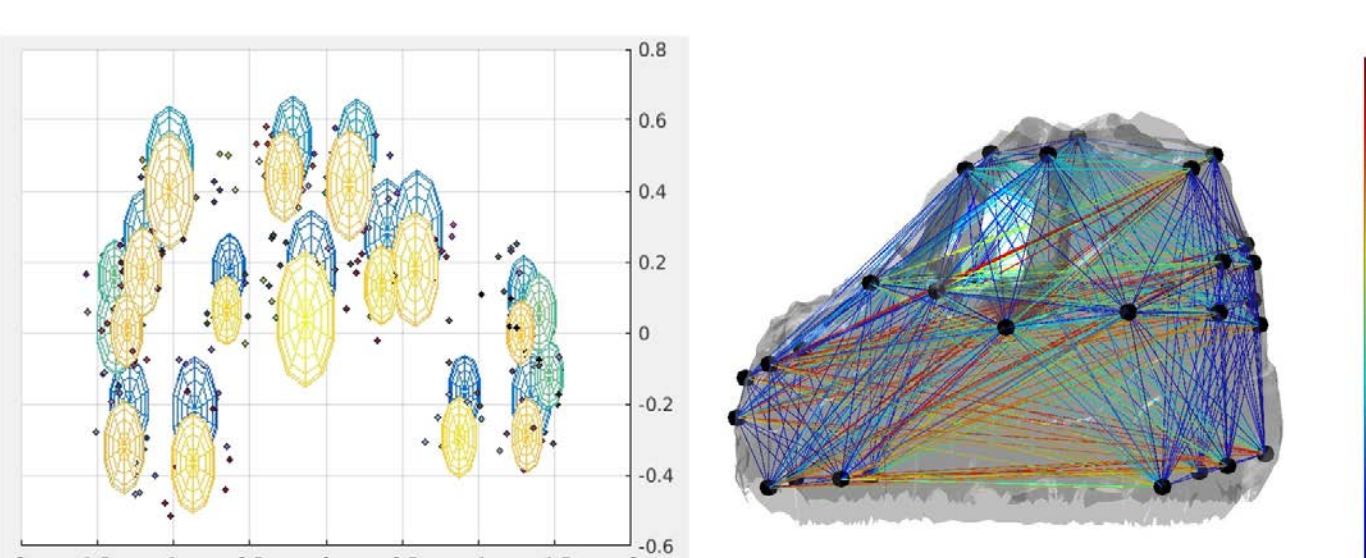


Figure 3: 3D Part Geometry. (Left) Std. Dev. of part locations. (Right) Variances in the mutual distance between each part pair overlaid on mean shape

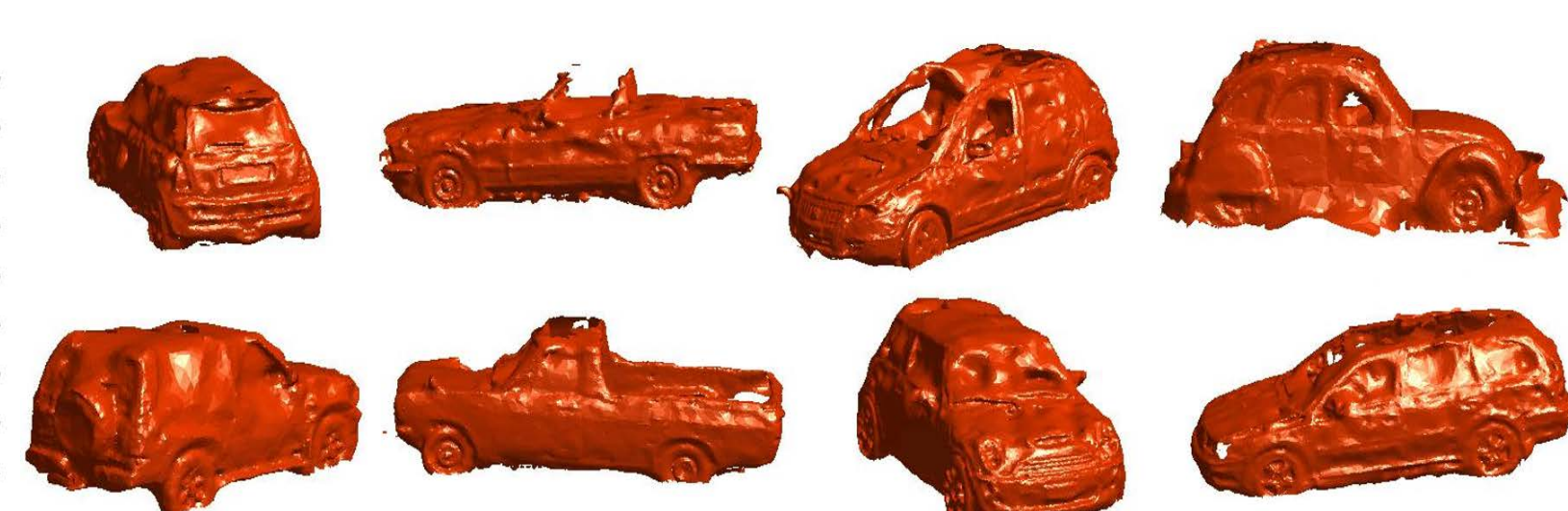


Figure 4: Training set examples: 3D meshes of RealCar Dataset.

## Algorithm 1: Shape recovery, pose estimation, detection

- *Part Detection*: SVM part appearance classifiers on conv5 feature pyramids, Non-Maxima Suppression + Platt's scaling.
- *Viewpoint Estimation*: Fit camera params for mean shape ( $|\text{min set}|=3$ , Algo. 2).
- *Viewpoint and Shape Refinement*: Repeat RANSAC-based routine by incrementally optimizing loss w.r.t. the 5 deformation bases and camera params ( $|\text{min set}|=5$ ).
- *Object Mask*: by projecting estimated deformable shape under estimated camera.

## Algorithm 2: RANSAC-based function estimation

- Do *Part detection* to obtain possible candidates.
- For  $N$  iterations do
  - Randomly sample jointly visible, minimal set of unique parts.
  - Fit unknown parameters by minimizing projection loss.
  - Check for inliers within threshold  $\tau_1$
  - If number of inliers greater than threshold  $\tau_2$  then store them
- Re-estimate params by minimizing proj. loss for the set with maximum inliers.

## EVALUATION

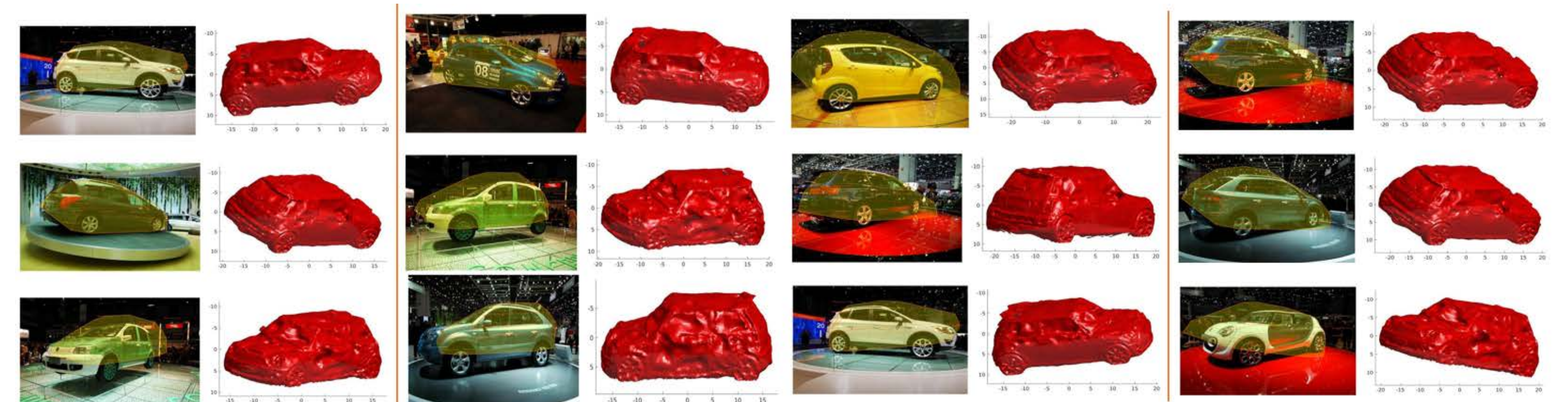


Figure 5: EPFL Cars: **Odd columns**: Test image + Viewpoint/Shape estimations overlaid, **Even columns**: Viewpoint Estimate using a sample mesh. Quantitative results below.

$\theta$	Our RealCar Dataset						EPFL Multi-view Cars Dataset						
	(Ours) Training Set			(Ours) Test Set			(Ours)			3D <sup>2</sup> PM[13]		Ozuysal et al. [28]	Glasner et al. [29]
	MPPE	MAE	MAE <sup>1</sup>	MPPE	MAE	MAE <sup>1</sup>	MPPE	MAE	MAE <sup>1</sup>	MPPE	MAE	MPPE	MAE
$\pi/4$	93.8	13.0	16.1	86.1	14.1	18.3	59.9	17.4	31.5	78.5	12.9	-	24.8
$\pi/6$	89.4	11.9	14.9	79.1	12.4	16.3	50.1	13.6	22.7	75.5	9.0	-	-
$\pi/8$	83.9	11.1	13.2	71.3	10.9	14.5	40.5	10.7	17.3	69.8	7.2	41.6	-
$\pi/9$	78.3	10.3	12.3	65.2	9.9	13.5	36.7	9.6	15.1	71.8	6.2	-	-
$\pi/18$	46.6	5.5	6.9	43.5	6.2	6.6	19.2	4.8	8.0	45.8	5.2	-	-

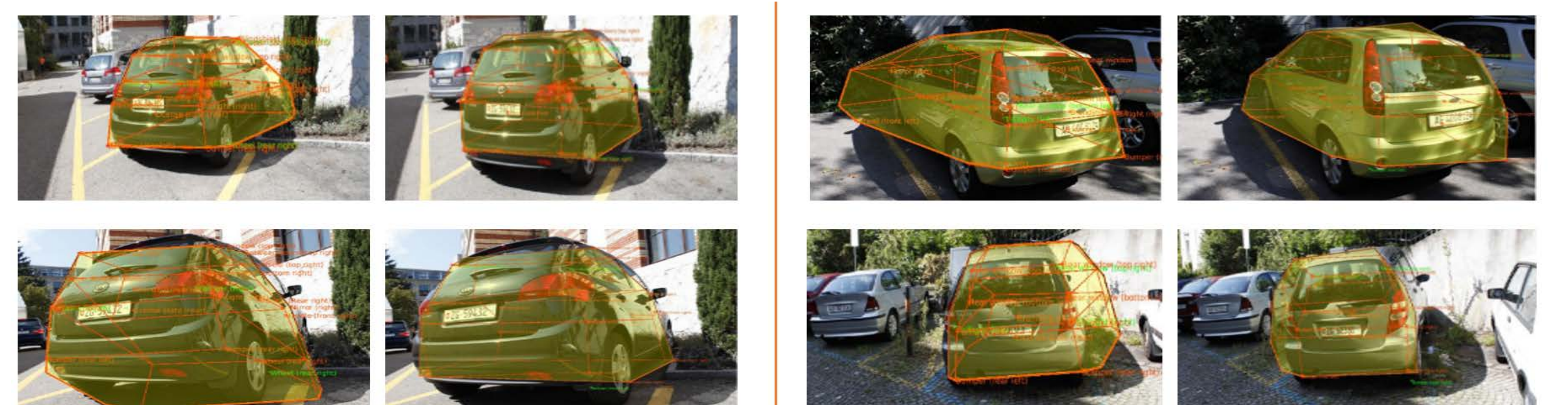


Figure 6: Improvement due to the Viewpoint and Shape refinement step

## SUMMARY

- Good results for class-specific shape and view reconstruction on state-of-the-art.
- Fine-grained parts and linear subspace representation model deformation effectively and true to life, but with far fewer vertices than full shape.
- Our method fast but still efficient and also models the projection process more accurately than regression, refinement step clearly helps.
- Aim: To explore unsupervised methods with more image evidence.